Published in final edited form as:
Annu Rev Biochem. 2009 ; 78: 701. doi:10.1146/annurev.biochem.78.070907.103812.

Mechanism of Mo-Dependent Nitrogenase

Lance C. Seefeldt[#,*], **Brian M. Hoffman**[†], and **Dennis R. Dean**[±]

Lance C. Seefeldt: lance.seefeldt@usu.edu; Brian M. Hoffman: bmh@northwestern.edu; Dennis R. Dean: deandr@vt.edu

[#] Department of Chemistry and Biochemistry, Utah State University, Logan Utah 84322

[±] Department of Biochemistry, Virginia Tech University, Blacksburg, Virginia 24061

[†] Department of Chemistry, Northwestern University, Evanston, Illinois 60208

Abstract

Nitrogen-fixing bacteria catalyze the reduction of dinitrogen (N_2) to two ammonia molecules (NH_3), the major contribution of fixed nitrogen into the biogeochemical nitrogen cycle. The most widely studied nitrogenase is the Mo-dependent enzyme. The reduction of N_2 by this enzyme involves the transient interaction of two component proteins, designated the Fe protein and the MoFe protein, and minimally requires sixteen MgATP, eight protons, and eight electrons. The current state of knowledge on how these proteins and small molecules together effect the reduction of N_2 to ammonia is reviewed. Included is a summary of the roles of the Fe protein and MgATP hydrolysis, information on the roles of the two metal clusters contained in the MoFe protein in catalysis, insights gained from recent success in trapping substrates and inhibitors at the active site metal cluster FeMo-cofactor, and finally, considerations of the mechanism of N_2 reduction catalyzed by nitrogenase.

Keywords

Nitrogen fixation; FeMo-cofactor; iron-sulfur; Fe protein; MoFe protein

INTRODUCTION

Nitrogen (N) is an essential element for all living organisms, being a constituent of proteins, nucleic acids, and many other biomolecules. The largest pool of nitrogen in the biosphere is atmospheric dinitrogen (N_2), but this chemically inert form is unusable by most living organisms (1). Consequently, most organisms must obtain their nitrogen in "fixed" forms such as proteins, ammonia, or nitrate. The input of N_2 into the biogeochemical nitrogen cycle occurs by reduction of N_2 yielding two ammonia molecules, which are subsequently converted into other usable forms of nitrogen. The majority of N_2 reduction (dinitrogen fixation) that occurs today, ultimately supporting the nitrogen demand of an estimated 60% of the human population, is by biological nitrogen fixation catalyzed by microorganisms, called diazotrophs (1). The remaining N_2 reduction is accomplished by the industrial Haber-Bosch process, requiring a metal (Fe-based) catalyst, H_2, and high pressures and temperature. The catalyst for biological N_2 reduction is the enzyme nitrogenase. It also utilizes a metal-based catalyst and a high energy input in the form of ATP, but functions at room temperature and atmospheric pressure (2).

*Corresponding author: Lance Seefeldt, Department of Chemistry and Biochemistry, Utah State University, 0300 Old Main Hill, Logan, UT 84322; ph. 435-797-3964, fax 435-797-3390, lance.seefeldt@usu.edu.

There are four known types of nitrogenases, with each encoded at the genetic level by a unique set of genes and each having a different combination of metals at the active site (2–4). The most abundant and widely studied nitrogenase group is the Mo-dependent enzyme, which has an active site metallo-cofactor called FeMo-cofactor (5). FeMo-cofactor contains Mo in addition to Fe, S, (*R*)-homocitrate, and a light atom of unknown identity called X (6). This review will focus on the current state of knowledge for the mechanism of this nitrogenase. The other so called "alternative nitrogenases" have been reviewed elsewhere (3).

The ideal reaction catalyzed by the Mo-dependent nitrogenase can be represented by the chemical equation (eqn 1):

$$N_2 + 8\,H^+ + 16\,MgATP + 8\,e^- \rightarrow 2\,NH_3 + H_2 + 16\,MgADP + 16\,P_i \qquad \text{(equ 1)}$$

The enzyme is composed of two-component metalloproteins called the iron (Fe) protein (also called dinitrogenase reductase or component II) and the molybdenum-iron (MoFe) protein (also called dinitrogenase or component I) (Figure 1). The structures of the two nitrogenase component proteins (individually and in complex with each other), have been determined by X-ray crystallography (6–25). These structures have provided detailed models of the three metal clusters contained in nitrogenase. The reduction of N_2 by nitrogenase involves a complex interplay between these two protein components, electrons, MgATP, and protons (26–30). Understanding the molecular details of this multi-step and multi-component system has proven to be challenging. This review summarizes recent progress in defining aspects of this complex system, while highlighting the many remaining challenges.

Fe PROTEIN

Fe protein cycle

The nitrogenase Fe protein serves to deliver electrons, one at a time, to the MoFe protein in a process coupled to the hydrolysis of two MgATP molecules (28,31). The Fe protein is a homodimer ($M_r \approx 64{,}000$) having one nucleotide (MgATP/MgADP) binding site buried within each subunit and a single [4Fe-4S] cluster bridging the two subunits (Figure 1) (13). The participation of the Fe protein in the nitrogenase mechanism can be considered to operate in a three state cycle (called the Fe protein cycle) (Figure 2, top). In this cycle, the reduced Fe protein, with its [4Fe-4S] cluster in the 1+ oxidation state, has two bound MgATP molecules. It is this state that transiently associates with the MoFe protein (32). During this association, the two MgATP molecules are hydrolyzed to two MgADP molecules, and a single electron is transferred from the Fe protein [4Fe-4S] cluster into the MoFe protein. The oxidized Fe protein ($[4Fe\text{-}4S]^{2+}$), now with two bound MgADP molecules, then dissociates from the MoFe protein in what is the overall rate-limiting step for nitrogenase catalysis (33). The released Fe protein is then regenerated in two steps. The MgADP molecules are replaced by MgATP, and the $[4Fe\text{-}4S]^{2+}$ cluster is reduced to the 1+ oxidation state, with the order of these two events being unclear (34). The physiological reductant for the Fe protein depends on the organism, with reduced ferredoxin or flavodoxin being the most common immediate electron donor (35,36).

Many questions remain about mechanistic details of the Fe protein cycle (28,31,37). For example, the specific nature of the communication between the nucleotide binding sites within the Fe protein and MoFe protein interface remain obscure. Prior to association with the MoFe protein, the Fe protein shows undetectable rates of MgATP hydrolysis. Once bound to the MoFe protein, the hydrolysis of MgATP is activated. Given that the MgATP binding sites within the Fe protein are located some distance away (> 10 Å) from the MoFe protein docking interface (13), this situation demands protein conformational changes induced within the Fe protein that activate MgATP hydrolysis (28,31). Two specific "switch" regions (stretches of

amino acids) within the Fe protein have been proposed to function to communicate between the docking interface and the MgATP binding site, resulting in movement of key catalytic residues that result in activation of nucleotide hydrolysis (7,15,20,22–24,38,39). Although broad strokes of this process have been defined, details of the mechanism remain unresolved. Likewise, little is known about how MgATP binding and hydrolysis within the Fe protein is communicated into the MoFe protein. That such a communication must occur is suggested by the observation that the Fe protein is the only known reductant for the MoFe protein that will support substrate reduction (2). An ability of small-molecule electron donors to reduce the MoFe protein without an attendant ability to support substrate reduction indicates that changes within the MoFe protein are induced by the Fe protein and must be coupled to MgATP hydrolysis. Other reviews provide a detailed historical perspective on the role of the Fe protein in nitrogenase catalysis (2,31,34,40).

MoFe PROTEIN

FeMo-cofactor

The MoFe protein is an$\alpha_2\beta_2$ heterotetramer ($M_r \approx 250{,}000$) that contains two pairs of novel metalloclusters, called P-cluster ([8Fe-7S]) and FeMo-cofactor ([7Fe-Mo-9S-homocitrate-X]). One of each type of metal cluster is contained in an αβ-unit (11,12), and thus each MoFe protein consists of two catalytic units (Figure 1). FeMo-cofactor is the site of substrate binding and reduction (Figure 3). This cofactor consists of a transition metal-sulfur framework and one molecule of (*R*)-homocitrate (41). A [4Fe-3S] subcluster is connected to a [3Fe-Mo-3S] subcluster by the atom X at one corner and three bridging inorganic sulfides (6). (*R*)-Homocitrate is coordinated to the Mo atom through its 2-hydroxy and 2-carboxyl groups. The presence of the light atom (X) at the center of FeMo-cofactor was detected in a high-resolution (1.16 Å) structure of the MoFe protein (6). The electron density for X is most consistent with N, C, or O, but efforts to identify this atom have yet to be successful (42–44). FeMo-cofactor is anchored to the MoFe protein byα-275^{Cys} to an Fe atom at one end and α-442^{His} to the Mo atom at the other end.

There is substantial evidence that FeMo-cofactor is the site of substrate binding and reduction. (**i**) Certain mutant strains that are deficient in FeMo-cofactor biosynthesis are inactive for reduction of all substrates, but can be activated by the addition of isolated FeMo-cofactor (45,46). (**ii**) MoFe protein that contains a structurally altered FeMo-cofactor, wherein citrate substitutes for homocitrate, exhibit altered catalytic properties (47–49). (**iii**) Amino acid substitutions in the FeMo-cofactor binding environment elicit changes in the catalytic and spectroscopic properties of the altered MoFe protein (29). (**iv**) In CO-inhibited MoFe protein, ENDOR spectroscopy shows that the CO binds to FeMo-cofactor, not to the P cluster (50–54).

P-cluster: role in catalysis

Each αβ-unit of the MoFe protein also contains one P-cluster. The P-clusters are [8Fe-7S] clusters (Figure 4) that are believed to mediate electron transfer between the Fe protein and the substrate reduction site FeMo-cofactor because of the following: (**i**) X-ray crystal structures of two different stable Fe protein-MoFe protein complexes place the P-cluster between the Fe protein [4Fe-4S] cluster and FeMo-cofactor (Figure 1) (7,8,55,56); (**ii**) Amino acid substitutions placed within the MoFe protein at positions between the P-cluster and the FeMo-cofactor perturb the intramolecular transfer of electrons from the P-cluster to FeMo-cofactor (57); (**iii**) Stopped-flow and EPR spectroscopic results obtained under turnover conditions indicate that the P-cluster is oxidized during the reduction of bound dinitrogen (58); (**iv**) Fe protein supports the MgATP-dependent transfer of an electron to the oxidized P-cluster of the MoFe protein; and finally (**v**) the P-clusters within a MoFe protein having the β-188^{Ser} residue

substituted by cysteine change oxidation state during turnover as indicated by freeze-quench EPR spectroscopy (59).

The P-cluster has a unique overall architecture, being constructed from two linked [4Fe-4S] subclusters that have a common bridging μ_6-sulfide at one corner (S1 in Figure 4) and is the only known naturally occurring [Fe-S] cluster that contains serinate-O (β-188^{Ser}) and amide-N (α-88^{Cys}) ligands, in addition to typical cysteinate-S ligands (11,60). X-ray crystallographic studies of two different oxidation states of the MoFe protein have revealed that P-clusters undergo structural rearrangement upon oxidation (P^{OX}) from the resting state (dithionite reduced; P^N), one consequence of which is the displacement of both the serinate-O and amide-N ligands from P^N (Figure 4) (60). The significance of these structural changes in the nitrogenase mechanism are not understood. It is known that treatment of the MoFe protein with small molecule electron transfer agents can induce different oxidation states of the P-cluster. In the P^N state, all of the Fe atoms are in the ferrous oxidation state (61,62) as determined by Mössbauer spectroscopy (eqn 2).

$$P^N \rightleftharpoons P^{1+} \rightleftharpoons P^{2+} \rightleftharpoons P^{3+} \quad \text{(equ 2)}$$

Reduction of the P^N state (to a hypothetical P^R state) has never been observed. Thus, it seems most reasonable to conclude that only P^N and more oxidized states are utilized during catalysis. Using mediators (62–64), the P^N state can be sequentially oxidized by three electrons, accessing the P^{1+}, P^{2+} (also called the P^{ox}), and P^{3+} oxidation states (eqn 2). The $P^{3+/2+}$ redox couple is not reversible *in vitro*, and thus it is concluded that this couple does not function *in vivo*. This suggests a model where the $P^{1+/N}$ and $P^{2+/1+}$ couples could be involved in P-cluster electron transfer, offering the possibility for transfer of one or two electrons from the P cluster to FeMo-cofactor during catalysis. The E_m values for these two couples are −300 mV (vs NHE) (65), similar to the E_m value for the [4Fe-4S] cluster in the Fe protein (−420 mM when MgATP is bound to the protein) (66). The P^N state of the P-cluster is EPR silent, whereas the P^{1+} and P^{2+} states are paramagnetic, with the P^{1+} state being a mixed spin system with S = 1/2 and 5/2 and the P^{2+} state being an S > 3 system with a perpendicular mode EPR signal (67). Despite being EPR-active, the P^{1+} and P^{2+} states have been difficult to detect in nitrogenase turnover samples, and there is little information about the oxidation states that the P-cluster accesses during turnover (68).

Based on the available information, a reasonable working model for P-cluster function can be suggested. In this model, the P-cluster in its all ferrous resting (P^N) state first transfers one or two electrons to FeMo-cofactor upon association of the Fe protein with the MoFe protein, and this is quickly followed by re-reduction of the oxidized P-cluster to the P^N state by electron transfer from the Fe protein. This model would explain the failure to observe P^{ox} states by EPR in turnover-trapped states, as the P^{ox} cluster would be transient and quickly reduced by the Fe protein. Experimental tests of this model are required.

MoFe protein cycle

During catalysis, the FeMo-cofactor must accept eight electrons (eqn 1), while only one electron is delivered during each Fe protein binding event. This process of accumulation of electrons by the MoFe protein and corresponding reduction of N_2 can be represented by a nomenclature for intermediate catalytic states of MoFe protein developed by Thorneley and Lowe (33). The number of electrons (and protons) added to the MoFe protein (E) is denoted n (Figure 2, bottom cycle), with MoFe protein thus proceeding through states from E_0 to E_8 during N_2 fixation before it returns to the E_0 (resting) state. The Fe protein 1-electron cycle and the MoFe protein 8-electron cycle can be thought of as interlocking, with the Fe protein

cycle (Figure 2, top cycle) driving the MoFe protein (Figure 2, bottom cycle) to successively reduced states.

This model for the nitrogenase mechanism illustrates several important observations about the mechanics of catalysis. For example, it is known that three or four electrons must accumulate within the MoFe protein before N_2 binds (E_3 or E_4 states) (33). Further, when N_2 binds to the MoFe protein, a stoichiometric quantity of H_2 is evolved (69,70). In the absence of N_2, the MoFe protein under turnover cycles through low E_n states while producing H_2. The reduction of protons by nitrogenase is one of the chief complications in attempts to accumulate an E_n state for study. In addition to reducing N_2 and protons, nitrogenase can reduce a number of small compounds containing double or triple bonds (Figure 5), with the reduction of the alkyne acetylene (C_2H_2) to ethylene (C_2H_4) being the most commonly used method for monitoring nitrogenase activity (2,71). The range of substrates utilized by nitrogenase has been reviewed elsewhere (2). It is worth noting that acetylene binds to a less-reduced E state (E_2) than does N_2 (E_3, E_4), and thus when acetylene and N_2 are both present, acetylene appears to be a non-competitive inhibitor of N_2 reduction, even though these two compounds are likely to bind to the same site on FeMo-cofactor. This is supported by the observation that N_2, which binds to more reduced states than does acetylene, is a competitive inhibitor of acetylene reduction (29).

DISCOVERING SUBSTRATE INTERACTION SITES

A genetic approach

Surprisingly, having the MoFe protein crystal structure in hand did not reveal an obvious and unique location for substrate binding and reduction on FeMo-cofactor. However, the structure of FeMo-cofactor (Figure 3) did suggest several possibilities. Among these included one or more of the six Fe atoms that comprise the waist region, Mo, or some combination of Fe, S, and Mo (30). Indeed, computational analysis conducted on FeMo-cofactor, or fragments of the cofactor, have suggested a wide range of potential substrate binding locations (30). Unfortunately, until recently, little information from studies on the enzyme was available to guide such studies. The x-ray structure, however, also suggests the way towards a solution. The central FeS portion of FeMo-cofactor is observed to be three-fold symmetric, with three equivalent 4Fe-4S faces, but the environment of FeMo-cofactor is not symmetric. Thus, it is clear that the protein environment must play a controlling role in defining the reactivity of FeMo-cofactor. This is most evident from the limited reactivity of FeMo-cofactor when it is removed from the protein into organic solvent, including a complete absence of N_2 reduction activity (72). Thus, it was reasonable to conclude that substitution of amino acids within the MoFe protein that are located near FeMo-cofactor might reveal the location of substrate binding.

Amino acids were targeted for substitution based on amino acid sequence conservation among nitrogenases from different organisms and by the location of the amino acid in the X-ray structure of the MoFe protein. Among the many MoFe protein substitutions made in the initial studies, the most interesting was one where the α-subunit 195^{His} residue is substituted by glutamine (73–77). Inspection of the X-ray crystal structure (14) reveals that the α-195^{His} residue is hydrogen bonded to one of the bridging S^{2-} atoms contained within the FeMo-cofactor (Figure 6). Biochemical characterization of the α-195^{Gln} substituted MoFe protein revealed that it does not significantly reduce N_2 (less than 1%) but is able to reduce acetylene just as effectively as the wild-type protein (73,76). Even though N_2 is not a substrate for the α-195^{Gln} substituted MoFe protein, N_2 remains as an inhibitor of both acetylene and proton reduction. The major conclusions from this work were that N_2 and acetylene compete for a common or shared binding site and that the α-195^{Gln} MoFe protein is unable to overcome a thermodynamic barrier necessary to accomplish N_2 reduction. It was not possible from these

studies, however, to infer the specific site of substrate binding. This is because substitution of α-195^{His} by glutamine is most likely to have affected N_2 reduction by altering the electronic properties of FeMo-cofactor. Namely, because N_2 reduction is more chemically demanding than acetylene reduction, electronic perturbations of FeMo-cofactor are likely to be manifested as a disruption in N_2 reduction without necessarily impacting acetylene reduction. Such perturbations could alter the electronic state of FeMo-cofactor or disrupt the transfer of electrons to FeMo-cofactor. Either effect could occur over long distance, and thus it is not possible to correlate the location of α-195^{His} with the site of substrate binding.

A different approach was needed to gain insights into the precise location of substrate binding. To accomplish this goal, a strategy was devised that relied on the prediction that an altered MoFe protein defective in acetylene reduction but not affected in N_2 reduction must have an altered active site that is able to discriminate between acetylene and N_2 (78). Such an altered protein could not be altered in electron transfer or electronic state because the reduction of N_2 – which would not be affected - is more difficult than acetylene reduction. The experimental challenge was to uncover such an altered MoFe protein. This was accomplished by taking advantage of the fact that acetylene is a potent physiological inhibitor of N_2 reduction. The strategy developed was to isolate a mutant strain of the dinitrogen fixing organism *Azotobacter vinelandii* that is resistant to acetylene inhibition of N_2 fixation-dependent growth (78). Considering that acetylene is only slightly larger than N_2 (Figure 5), it would have been impossible to rationally design the appropriate residue position for substitution. Thus, the beauty of the genetic approach was that the organism did all of the difficult work by simple genetic selection.

A number of spontaneous acetylene-resistant mutants were isolated and characterized, and all of them had substitutions at the α-69^{Gly} position (78). For these substituted MoFe proteins, the V_{max} and K_m for N_2 reduction were unchanged, whereas the K_m for acetylene reduction had increased 20-fold (79). The α-69^{Gly} residue is located in the second shell of amino acids away from those directly interacting with the FeS face at the waist of FeMo-cofactor(Figure 6). An adjacent amino acid in the α-chain is α-70^{Val}, the side-chain of which approaches one of the three ‘4Fe-4S’ faces of FeMo-cofactor. This FeS face of FeMo-cofactor involves Fe atoms 2, 3, 6, and 7 (using the numbering scheme in the PDB file 1M1N). Because α-69^{Gly} is not close enough to directly influence substrate binding, it is more reasonable to expect that substitutions placed at the α-69^{Gly} position might alter the dynamic movement of the α-70^{Val} side-chain thereby permitting the discrimination between acetylene and N_2 or effective access to this 4Fe face. This work provided the first direct experimental evidence that initial substrate binding for both acetylene and N_2 can occur at a specific Fe-S face of FeMo-cofactor.

Altering the substrate size range

The FeS face of FeMo-cofactor hypothesized to be the site of reduction is directly approached by the side chain of α-70^{Val}. This suggested a model wherein the side chain of this residue might impose steric constraints on the size of substrates that could gain access to the active site. To test this hypothesis, the α-70^{Val} was substituted by amino acids having either larger (Ile) or smaller (Ala or Gly) side chains (Figure 7) and the ability of the substituted MoFe proteins to reduce substrates of different sizes was tested (80–84). It was predicted that substitution of the larger side chain of α-70^{Ile} might block access of substrates, whereas substitution by the smaller side chain α-70^{Ala} might open access to the active site and thereby permit larger compounds that are not normally substrates to become substrates for nitrogenase. A series of kinetic studies supported this model (80–85). The α-70^{Ala} MoFe protein was found to reduce propyne and propargyl alcohol (Figure 5) at considerable rates, whereas the α-70^{Val} (wild-type) MoFe protein did not. It was also found that the α-70^{Ala} substituted MoFe protein can reduce hydrazine (H_2N-NH_2) at high rates, whereas the wild-type does not (86).

Substitution of α-70^{Val} by the smaller Gly residue also endowed the MoFe protein with an ability to reduce an even larger alkyne substrate, 1-butyne, at measureable rates (84). In a complementary experiment, the α-70^{Ile} substituted MoFe protein was found to reduce only protons at normal rates (validating the catalytic integrity of the active site), with limited reduction rates for acetylene, N_2, or hydrazine (87). These findings reveal two critical aspects about substrate interactions with nitrogenase: **(i)** both alkyne and nitrogenous substrates, including acetylene and N_2, have the capacity to interact with the same FeS face of FeMo-cofactor that is approached by the α-70^{Val} side chain and **(ii)** the substrate range of nitrogenase can be controlled by manipulation of the side chain located at the α-70 residue position.

While the studies described above narrowed the location of interaction for both alkyne and nitrogenous substrates to a specific FeS face of FeMo-cofactor, they did not predict a specific site for binding. Additional studies helped to further localize the binding location for alkyne substrates. One study took advantage of the observation that propargyl alcohol is a substrate for the α-70^{Ala} substituted MoFe protein and that during turnover with this substrate, a novel EPR active state could be trapped by rapidly freeze-quenching (81,83). As described below, through use of electron nuclear double resonance (ENDOR) spectroscopy, it was possible to demonstrate that this EPR spectrum results from FeMo-cofactor that has a reduction product of propargyl alcohol bound side-on to a single Fe (alkene π complex or a ferracycle) (80). This finding represented the first determination of the structure of a substrate-derived species trapped on FeMo-cofactor.

Important to localizing the site of interaction of this intermediate were the observations that while propargyl alcohol could be trapped, propyne (Figure 5) could not be trapped, and that α-195^{His}, which is located on the same FeS face under α-70^{Val} (Figure 6), participated in trapping the propargyl alcohol intermediate. By examining the pH dependence for trapping the intermediate, substituting amino acids for α-195^{His}, and using propargyl amine (Figure 5) as another trapped substrate, it became clear that one or more of the four Fe atoms (2, 3, 6 and 7) was the site of substrate interaction (81). Molecular dynamic modeling was then used to predict specifically which of the four Fe atoms was the most likely site for the alkene binding. These calculations also supported the conclusion from spectroscopic studies for side-on binding of the intermediate to Fe6.

Another study started from the observation that binding of alkynes to Fe6 would place the side chain of α-191^{Gln} within Van der Waals contact with the bound substrate (Figure 6) suggesting that the side chain of this residue might exclude larger substrates from gaining access to the active site (84). To test this possibility, a doubly substituted MoFe protein was constructed having substitutions at the α-70^{Val} and α-191^{Gln} positions. Substitution of α-70^{Val} by alanine endows the resulting MoFe protein with an ability to reduce the larger alkyne 1-butyne (Figure 5), whereas the α-70^{Val} MoFe protein is unable to reduce this alkyne. The α-70^{Ala} MoFe protein is unable, however, to reduce the internal alkyne, 2-butyne, as predicted because of steric conflict between the methyl group of the substrate and the side chain of α-191^{Gln} (84). To test this possibility, the side chain of α-191^{Gln} was substituted by the smaller amino acid alanine in combination with the α-70^{Ala} substitution. This MoFe protein was found to reduce 2-butyne at appreciable rates, consistent with the reaction of this substrate at Fe6 of FeMo-cofactor.

From the series of studies summarized above, several conclusions can be drawn about the interaction of substrates with nitrogenase: (**i**) both nitrogenous (N_2 and hydrazine) and alkyne (e.g., acetylene and propyne) substrates interact with the same site on FeMo-cofactor, (**ii**) the side chain of α-70^{Val} controls access of substrates to the site of interaction, which logically must encompass Fe atoms 2, 3, 6, and 7, (**iii**) alkyne substrates are proposed to interact specifically with Fe atom 6. These studies provided the first general localization of the site of substrate interactions with the nitrogenase active site. However, they provided no information

about the potential for migration of bound intermediates between metal atoms during reduction, or about the intermediates occurring along the N_2 reaction pathway. These latter points require the trapping and characterization of multiple intermediates bound to FeMo-cofactor.

INTERMEDIATES TRAPPED ON FeMo-COFACTOR

Inhibitors

There are many challenges to trapping species on FeMo-cofactor. Key among these is the requirement that only reduced states of the MoFe protein are able to bind either inhibitors or substrates (2). This necessitates that carefully controlled turnover conditions must be achieved before substrates can bind, with the return to the resting state occurring with H_2 being evolved. The need for active turnover coupled with a complex multistep reaction pathway makes it difficult to populate a single state that would be suitable for characterization by spectroscopic techniques. This problem was partially overcome by using the inhibitor CO (88). CO inhibits all substrate reductions by nitrogenase except proton reduction (88,89). When CO is added to nitrogenase under steady-state turnover conditions and the sample is frozen in liquid nitrogen, the enzyme can be trapped in states having characteristic EPR spectra (50–54,90). Three different EPR signals are observed depending on the concentration of CO used (designated as “lo CO”, “hi CO”, and ”hi(5) CO”). By using ^{13}CO, coupled with ENDOR spectroscopy, considerable insight into the nature of the CO bound states was obtained (50–54). Key conclusions from these studies were that the observed paramagnetic species arises from FeMo-cofactor and that the lo CO bound state involves a single CO molecule bound end-on bridging between two Fe atoms of FeMo-cofactor. For the hi CO state, two CO molecules were proposed bound end-on to two separate Fe atoms.

Alkyne substrates

The next challenge was to devise ways to trap states formed during substrate turnover in sufficient concentration for detailed characterization. An early success was realized by trapping a state formed during reduction of propargyl alcohol in the α-70^{Ala} MoFe protein, as already described (80–83). When the α-70^{Ala} substituted MoFe protein was frozen in liquid nitrogen during steady-state turnover using propargyl alcohol as the substrate, the S = 3/2 EPR spectrum of the FeMo-cofactor was observed to change to a new S = 1/2 spectrum (Figure 8). Using ^{13}C-propargyl alcohol and ^{13}C-ENDOR spectroscopy, it was subsequently possible to demonstrate that the new EPR signal originates from FeMo-cofactor having a bound propargyl alcohol derivative. Through a series of $^{1,2}H$-ENDOR studies on this state, it was possible to generate a list of constraints on the structure of this trapped intermediate (80). Tests of these constraints against all known structures of small molecule metal-alkyne/alkene complexes suggested that the state contained an allyl alcohol ($H_2C{=}CH{-}CH_2OH$) bound side-on to a single Fe atom. The characterization of this trapped state was important for several reasons. It was the first substrate-derived intermediate bound to FeMo-cofactor that was characterized at the molecular level and it also revealed how best to use ENDOR-derived constraints to deduce structure. Second, it provided insights into how additional substrates, including nitrogenous substrates, could be trapped under turnover conditions. Essential among the lessons learned was that substitution of amino acids near FeMo-cofactor could be used in combination with rapid-freezing during turnover to trap intermediates in high concentration. This approach was used to trap an intermediate during acetylene reduction and application of EPR and ENDOR spectroscopy revealed a trapped state similar to that described for propargyl alcohol (91).

Proton intermediate

In the absence of other substrates, all of the electrons passing through nitrogenase under turnover conditions (usually referred to as electron flux) are used for proton reduction (92). When N_2 is present, no less than 25% of the electron flux goes to proton reduction, with no

more than 75% going to N_2 reduction (eqn 1) (70). As described earlier, it was found that substitution of α-70^{Val} by the larger side chain amino acid isoleucine results in a MoFe protein that is blocked in the reduction of all substrates except protons (87). When this MoFe protein is trapped by freezing in liquid nitrogen during steady-state proton reduction, the FeMo-cofactor EPR spectrum exhibits a unique S = 1/2 EPR signal (Figure 8). By capturing this state in the presence of either H_2O or D_2O, and by using ^{1,2}H-ENDOR measurements, it was established that this signal arises from FeMo-cofactor with two $H^{+/-}$ bound, most likely as Fe-bound hydrides.

Nitrogenous substrates

Very little is known about the pathway and intermediates involved in N_2 reduction by nitrogenase. Early studies revealed that acid or base quenching of nitrogenase during turnover with N_2 resulted in a very small quantity of hydrazine (H_2N-NH_2) that could be detected (93). This result was interpreted as evidence for the existence of a bound intermediate at the level of reduction of hydrazine along the reaction pathway that would not normally escape FeMo-cofactor during the reaction. Beyond this early observation, there was little direct information about the nature of the intermediates along the reaction pathway. Several logical assumptions, however, can be proposed. For example, it is reasonable to assume that N_2 binds to one or more of the metal atoms in FeMo-cofactor followed by sequential addition of e^-/H^+ with the partially reduced intermediates remaining bound to one or more of the metal ions. Within that assumption, it is not widely recognized that there are two classes of reduction pathway that are distinguishable by the site of hydrogenation on bound N-N fragments (94, 95), with Figure 9 showing two limiting pathways, as is now discussed.

A starting point for the nitrogenase reaction pathway can be proposed from the mechanism for N_2 reduction catalyzed by organometallic complexes. The best characterized of such reactions is the Chatt mechanism for N_2 reduction on a mononuclear Mo metal complex (96,97), as elaborated with the recent observation of catalytic reduction by Mo complexes by the Schrock group (98–102). The essential intermediates in this reaction pathway are shown in Figure 9 (left). N_2 is bound to Mo (represented as M) followed by stepwise reduction and proton addition, with each intermediate remaining bound to the metal. N_2 is successively hydrogenated at a single ('distal') N until the N-N bond is cleaved after the addition of 3 e^-/H^+, with release of the first ammonia. The second ammonia is released following further reduction of the bound nitrido species by 3 e^-/H^+. This has been denoted a distal (D) pathway because as drawn the distal N atom is protonated first and then released as NH_3 (94,95). But nitrogenase need not follow a similar reaction mechanism, and an alternative type of reaction pathway proposed for nitrogenase (Figure 9, right) is supported by several theoretical studies (30). Termed the alternating (A) pathway, the two N atoms are reduced alternately, with cleavage of the N-N bond occurring only later in the reaction (94). While both pathways involve the stepwise reduction of the N_2 bound to a metal, the alternating one provides for the addition of protons to both N atoms in turn, delaying cleavage of the N-N bound and release of the first ammonia molecule until after the addition of 5 e^-/H^+. A significant step toward defining the nitrogenase pathway would be to trap intermediate states bound to FeMo-cofactor during N_2 reduction and then to use the information gained from characterization of these states.

Key intermediates along the pathway of N_2 reduction by nitrogenase are proposed to be at the levels of reduction of metal bound diazene (HN=NH) and hydrazine (H_2N-NH_2) (Figure 9). During the last several years, strategies have been devised that allow states of the MoFe protein to be trapped starting from N_2, diazene (and methyldiazene), and hydrazine (103). Early characterization of these states assigned them as early (N_2), middle (diazene), and late (hydrazine) intermediates along the reaction sequence, whereas more recent work has suggested that diazene and hydrazine as substrates converge to a common state (95).

Hydrazine

As described earlier, hydrazine is a substrate for nitrogenase, being reduced to two ammonia molecules (104). Substituting α-70^{Val} by alanine results in a MoFe protein that has a significantly higher rate of hydrazine reduction compared to the wild-type MoFe protein (82, 86). Attempts to trap an intermediate bound to FeMo-cofactor during reduction of hydrazine by this MoFe protein variant were not successful. What was needed was some method for arresting the reaction so as to populate an intermediate in high concentration. Based on the earlier work illustrating that α-195^{His} is likely to approach the substrate binding site (Figure 6) (81,86), it was suggested that this residue might function to deliver protons during the reduction reaction (73). If true, it was then reasoned that substituting a glutamine for this residue might interrupt the delivery of protons for hydrazine reduction, resulting in the accumulation of a species bound to FeMo-cofactor. This prediction turned out to be correct as it was found that turnover of a doubly-substituted MoFe protein (α-70^{Ala}/α-195^{Gln}) with hydrazine generates a new state with a rhombic S = 1/2 EPR signal (> 60% of the total FeMo-cofactor signal (Figure 8) (82,86). Pulsed ENDOR spectroscopy using uniformly ^{15}N-labeled hydrazine revealed that the trapped intermediate was a hydrazine-derived species bound to FeMo-cofactor with a single type of ^{15}N signal. ^{1,2}H-ENDOR spectroscopy further showed that strongly coupled proton(s) were associated with the bound N, consistent with a FeMo-cofactor-N_yH_x species (103). The single observed N bound could result from end-on binding of hydrazine or from a single N atom fragment of hydrazine after N-N bond cleavage.

Diazene

The second alternate substrate that should access the N_2 reduction pathway is diazene (HN=NH). Diazene is very unstable, with a very short half-life in aqueous solutions, so a more stable derivative, methyldiazene (HN=N-CH_3), was first used in its place (94); subsequently, diazene generated *in situ* was used (95). Both diazene and methyldiazene are substrates for nitrogenase.

Again, the challenge was to figure out a way to trap intermediates at high concentration during turnover. As was the case for hydrazine, substituting the α-195^{His} residue for a glutamine was predicted to disrupt the delivery of protons required to complete substrate reduction. When the α-195^{Gln} MoFe protein was frozen during turnover in the presence of methyldiazene, the FeMo-cofactor EPR spectrum was observed to change to a unique S = ½ EPR signal (Figure 8) (94). By trapping the appropriately (^{15}N or ^{13}C) labeled substrates combined with application of ^{1}H-, ^{15}N-, and ^{13}C-ENDOR spectroscopies, several key features of the bound state were deduced: **(i)** a methyldiazene-derived species is bound to FeMo-cofactor; **(ii)** the bound species is an –N_yH_x fragment; and **(iii)** if y = 2, then only the terminal N atom is bound to FeMo-cofactor (94). When diazene was then trapped on the MoFe protein, a state with a slightly different EPR signal was observed (95). Comparison of the EPR, ^{1,2}H-, and ^{15}N-ENDOR spectra for this state with those of the hydrazine-derived intermediate strongly suggested that during turnover the diazene had ‘caught up’ to the hydrazine, and that the two states are the same (95).

N_2

Trapping a state under N_2 turnover required a different strategy than was used to trap one with methyldiazene or hydrazine. For the latter two substrates, proton delivery was disrupted by substitution of the α-195^{His} residue by glutamine. This substituted MoFe protein, however, showed little sign of trapping of an N_2-derived state. Instead, it was discovered that altering the electron flux through the wild-type nitrogenase could be used to trap a state during N_2 reduction (103). The electron flux (or rate of electron flow) through nitrogenase is controlled by altering the ratio of Fe protein to MoFe protein, with low ratios resulting in low electron flux and high ratios resulting in high electron flux. As the electron flux through nitrogenase is

decreased, the specific activity for N_2 and proton reduction is observed to decrease. It was found that at lower electron flux (2 Fe protein:1MoFe protein), a new S = 1/2 EPR state could be trapped when samples are frozen during steady-state turnover with N_2 (Figure 8). Initial ^{15}N-ENDOR analysis of this $^{15}N_2$-trapped state confirmed that the EPR signal arises from FeMo-cofactor with an N_2-derived species bound (103). The absence of an exchangeable ^{1}H signal(s) confirmed this intermediate is a less-reduced state than are the hydrazine/diazene states. The presence of only a single type of ^{15}N signal would be consistent with end-on binding of N_2 to FeMo-cofactor. The expected presence of the distal N atom has yet to be established.

CONSIDERATIONS OF MECHANISM

Approaching the mechanism

As described in the preceding sections, progress has been made in trapping three different nitrogenous substrates on FeMo-cofactor (103). These trapped states now must be mapped onto the nitrogenase E_n kinetic scheme (Figure 2) and N_2-reduction reaction pathway (Figure 9). While the characterization of the hydrazine, methyldiazene, and N_2 trapped states has just begun, several insights regarding the nitrogenase mechanism have already emerged (103). For all three substrates, ENDOR spectroscopy reveals a single N-species bound to FeMo-cofactor. The use of ^{1,2}H and ^{14,15}N ENDOR to determine the structures of the trapped nitrogenous reduction intermediates is a much more formidable task than was the determination of the structure of the alkyne reduction intermediates. Firstly, there are six stages of N_2 reduction, not two. Secondly, when alternative reaction pathways are taken into account (Figure 9), there are numerous possible $[N_xH_y]$ species to be considered at every stage of N_2 reduction. The N_2H_y (y = 0, 2, 4) substrates used are all symmetric, so selective labeling of the N's is impossible; all the N-H are solvent exchangeable, so selective deuteration is impossible. On the other hand, just a few ENDOR-derived constraints can act as a powerful means of narrowing the list of candidates: **(i)** is the N-N bond broken, and if not, are the two N's equivalent; **(ii)** what is the reduction level of the bound fragment (what is x); **(iii)** what is the binding mode if y = 2? Some of these constraints will come directly from ENDOR results for the intermediate states, but some from relaxation measurements to be described below.

The limited current information about the trapped states already tends to favor the alternating reaction pathway (Figure 9). One important observation is that there is no obvious entry point for hydrazine into the distal pathway, whereas there is in the alternating pathway. Assuming that the mechanism of hydrazine reduction is the same as the terminal stages of N_2 reduction, this would seem to favor the alternating pathway for nitrogenase.

One way to gain insights into the nature of the trapped substrate-derived intermediate and its position on the reaction pathway would be to convert one intermediate into another by a controlled reaction, analogous to the case of the diazene/hydrazine state. An approach towards connecting the trapped states with the kinetic scheme of Figure 9 has been recently reported (105). The approach is to use a temperature step annealing of the trapped states as a way to gradually and systematically observe a trapped intermediate relax while monitoring the appearance of new intermediates and ultimately the reappearance of the FeMo-cofactor resting state. By conducting these step-annealing studies in a frozen solid, the complication of additional electrons being delivered by the Fe protein is eliminated by preventing the Fe protein-MoFe protein association/dissociation. The basic approach is to warm a trapped state sample, which is stable at 77 K, to a temperature where it is still frozen (< 273 K) but where internal protein conformational changes and electron transfer can occur. The sample is held at this annealing temperature for a fixed period of time and then it is returned to 77 K, followed by analysis with EPR and ENDOR spectroscopies (conducted at 2–12 K). By performing a series of such steps, it is possible to determine the kinetics for the transformation of the trapped

state to new trapped states and ultimately back to the resting state. Testing for kinetic isotope effects on the reactions reveals steps that involve H^+ transfer and H_2 release, and may unmask hidden intermediates.

This protocol was first used to study the $H^{+/-}$ trapped state in the α-70^{Ile} substituted MoFe protein (105). At 253 K in the frozen state, this trapped state decays with a half-life of ~13 min. When this experiment was conducted in the presence of 85% D_2O instead of H_2O, the half-life increased to ~49 min, revealing a strong kinetic isotope effect on the decay reaction (KIE ~ 4). The decay of the proton-trapped state follows an A → B → C reaction mechanism, where A is the proton intermediate and C is the resting state FeMo-cofactor, and B represents a new high-spin paramagnetic species. The B → C step shows a similarly large KIE. The KIE in both steps was interpreted to indicate the generation of H_2 during the relaxations, an overall loss of four electrons from A. According to the scheme of Figure 2, this intermediate must then be the catalytically central E_4 state that is competent for N_2 binding and reduction by the accumulation of n = 4 electrons. Its relaxation by loss of H_2 generates the previously unobserved state B = E_2, and this relaxes with loss of H_2 to the resting state, C = E_0. With the successful application of this approach to the proton-trapped state, the stage is set to conduct similar experiments on the substrate trapped states, including hydrazine, methyldiazene, diazene, and N_2. Such studies, in combination with ENDOR measurements, offer the real prospect of better defining the exact state of each trapped species and the possible connection between each state, and of discriminating between distal and alternating pathways (Figure 9). Thus, one can anticipate powerful new insights into the nitrogenase mechanism.

From the discussion presented here, it should be evident that considerable progress has been made in understanding some aspects of the structure and function of nitrogenase. The most recent progress in trapping and characterizing substrate bound states is offering the first real glimpses into the N_2 reduction mechanism, but clearly the lion's share of the discoveries for this complex metalloenzyme lie in the future.

SUMMARY POINTS

1. All substrates for nitrogenase appear to bind to a single FeS face of FeMo-cofactor approached by the MoFe protein amino acid α-70^{Val}.
2. The binding of different substrates to the same site within FeMo-cofactor, but at different redox states, can explain the non-reciprocity with respect to their competition for occupancy of the active site.
3. A combination of amino acid substitution and rapid freezing has proven successful for trapping a number of alkyne and nitrogenous substrates on FeMo-cofactor.
4. The state trapped during reduction of the alkyne substrate propargyl alcohol contains a reduced form of the substrate bound to FeMo-cofactor. ^{13}C- and $^{1/2}H$-ENDOR spectroscopy indicate that this is the allyl-alcohol ($HO-CH_2-CH=CH_2$) reduction product bound side-on to one Fe6.
5. Species-derived from the four substrates hydrazine, methyldiazene, diazene, and N_2 have been trapped on FeMo-cofactor and spectroscopic analysis reveals that each is bound to FeMo-cofactor through a single type of N, with the N_2 intermediate at an earlier level of protonation.
6. A temperature step-annealing relaxation kinetics method has been applied to the proton trapped state, revealing this state likely has been activated for N_2 binding and reduction by the accumulation of four electrons (and protons).

7. The application of temperature step annealing and ENDOR spectroscopy to the other substrate trapped states offers the possibility of further defining the N_2 reduction reaction pathway and nitrogenase mechanism.

FUTURE ISSUES

1. A molecular level understanding of how MgATP hydrolysis is coupled to substrate reduction catalyzed by nitrogenase remains to be established.
2. The functional oxidation states and order of electron transfer involving the P-clusters remains to be solved.
3. It remains to be established if the N_2, diazene, and hydrazine states that have been trapped are on the N_2 reaction pathway and if the N-N bonds have been broken in each.
4. Studies over the coming years need to define the reaction intermediates and begin to narrow the possible mechanisms for N_2 reduction by nitrogenase.
5. Synthetic models of FeMo-cofactor that can reduce known nitrogenase substrates would be valuable in better understanding the reactivity of N_2 reduction.

Acknowledgments

The authors recognize financial support for their work from the National Institutes of Health (GM59087 to LCS; HL 13531 to BMH) and the National Science Foundation (MCB 0723330 to BMH; MCB-0717710 to DRD).

TERMS/DEFINITIONS

Fe protein	nitrogenase iron-protein, also called dinitrogenase reductase or component II
MoFe protein	nitrogenase molybdenum-iron protein also called dinitrogenase or component I
FeMo-cofactor	the iron-molybdenum cofactor bound in the MoFe protein having composition [7Fe-Mo-9S-homocitrate-X]. The site of substrate binding and reduction in nitrogenase
P-cluster	the iron-sulfur cluster bound in the MoFe protein having composition [8Fe-7S]. Presumed to mediate electron transfer from the Fe protein to FeMo-cofactor
EPR	electron paramagnetic resonance. A spectroscopic method that detects unpaired electrons or radicals. Valuable in detecting electronic or oxidation state changes in metal clusters
ENDOR	electron nuclear double resonance. A spectroscopic method that detects nuclear spins (e.g., ^{13}C or ^{15}N) that are coupled to electron spins (e.g., in metal cofactors in proteins). The method provides information about binding, electronic changes, and oxidation state changes associated with substrates or inhibitors binding to active site metal clusters

LITERATURE CITED

1. Smil, V. Enriching the Earth: Fritz Haber, Carl Bosch, and the Transformation of World Food Production. Cambridge, MA: MIT Press; 2001.
2. Burgess BK, Lowe DJ. The mechanism of molybdenum nitrogenase. Chem Rev 1996;96:2983–3011. [PubMed: 11848849]

3. Eady RR. Structure-function relationships of alternative nitrogenases. Chem Rev 1996;96:3013–30. [PubMed: 11848850]
4. Ribbe M, Gadkari D, Meyer O. N_2 fixation by Streptomyces *thermoautotrophicus* involves a molybdenum- dinitrogenase and a manganese-superoxide oxidoreductase that couple N_2 reduction to the oxidation of superoxide produced from O_2 by a molybdenum-CO dehydrogenase. J Biol Chem 1997;272:26627–33. [PubMed: 9334244]
5. Shah VK, Brill WJ. Isolation of an iron-molybdenum cofactor from nitrogenase. Proc Natl Acad Sci USA 1977;74:3249–53. [PubMed: 410019]
6. Einsle O, Tezcan FA, Andrade SLA, Schmid B, Yoshida M, et al. Nitrogenase MoFe-protein at 1.16 angstrom resolution: A central ligand in the FeMo-cofactor. Science 2002;297:1696–700. [PubMed: 12215645]
7. Chiu H-J, Peters JW, Lanzilotta WN, Ryle MJ, Seefeldt LC, et al. MgATP-bound and nucleotide-free structures of a nitrogenase protein complex between the Leu 127-Delta-Fe-protein and the MoFe-protein. Biochemistry 2001;40:641–50. [PubMed: 11170380]
8. Schindelin H, Kisker C, Schlessman JL, Howard JB, Rees DC. Structure of ADP-AlF_4-stabilized nitrogenase complex and its implications for signal transduction. Nature 1997;387:370–76. [PubMed: 9163420]
9. Kim J, Woo D, Rees DC. X-ray crystal structure of the nitrogenase molybdenum-iron protein from *Clostridium pasteurianum* at 3.0-Å resolution. Biochemistry 1993;32:7104–15. [PubMed: 8393705]
10. Chan MK, Kim J, Rees DC. The nitrogenase FeMo-cofactor and P-cluster pair: 2.2 Å resolution structures. Science 1993;260:792–94. [PubMed: 8484118]
11. Kim J, Rees DC. Structural models for the metal centers in the nitrogenase molybdenum-iron protein. Science 1992;257:1677–82. [PubMed: 1529354]
12. Kim J, Rees DC. Crystallographic structure and functional implications of the nitrogenase molybdenum iron protein from *Azotobacter vinelandii*. Nature 1992;360:553–60.
13. Georgiadis MM, Komiya H, Chakrabarti P, Woo D, Kornuc JJ, Rees DC. Crystallographic structure of the nitrogenase iron protein from *Azotobacter vinelandii*. Science 1992;257:1653–59. [PubMed: 1529353]
14. Sørlie M, Christiansen J, Lemon BJ, Peters JW, Dean DR, Hales BJ. Mechanistic features and structure of the nitrogenase alpha-Gln195 MoFe protein. Biochemistry 2001;40:1540–49. [PubMed: 11327812]
15. Jang SB, Seefeldt LC, Peters JW. Insights into nucleotide signal transduction in nitrogenase: Structure of an iron protein with MgADP bound. Biochemistry 2000;39:14745–52. [PubMed: 11101289]
16. Mayer SM, Gormal CA, Smith BE, Lawson DM. Crystallographic analysis of the MoFe protein of nitrogenase from a *nifV* mutant of *Klebsiella pneumoniae* identifies citrate as a ligand to the molybdenum of iron molybdenum cofactor (FeMoco). J Biol Chem 2002;277:35263–66. [PubMed: 12133839]
17. Mayer SM, Lawson DM, Gormal CA, Roe SM, Smith BE. New insights into structure-function relationships in nitrogenase: A 1.6 Å resolution X-ray crystallographic study of *Klebsiella pneumoniae* MoFe-protein. J Mol Biol 1999;292:871–91. [PubMed: 10525412]
18. Bolin, JT.; Ronco, AE.; Mortenson, LE.; Morgan, TV.; Williamson, M.; Xuong, NH. Nitrogen Fixation: Achievements and Objectives. Gresshoff, PM.; Roth, LE.; Stacey, G.; Newton, WE., editors. New York: Chapman and Hall; 1990. p. 117-22.
19. Bolin, JT.; Campobasso, N.; Muchmore, SW.; VMT; Mortenson, LE. Molybdenum Enzymes, Cofactors and Model Systems. Stiefel, EI.; Coucouvanis, D.; Newton, WE., editors. Washington DC: ACS; 1993. p. 186-95.
20. Sarma R, Mulder DW, Brecht E, Szilagyi RK, Seefeldt LC, et al. Probing the MgATP-bound conformation of the nitrogenase Fe protein by solution small-angle X-ray scattering. Biochemistry 2007;46:14058–66. [PubMed: 18001132]
21. Sen S, Krishnakumar A, McClead J, Johnson MK, Seefeldt LC, et al. Insights into the role of nucleotide-dependent conformational change in nitrogenase catalysis: Structural characterization of the nitrogenase Fe protein Leu127 deletion variant with bound MgATP. J Inorg Biochem 2006;100:1041–52. [PubMed: 16616373]

22. Sen S, Igarashi R, Smith A, Johnson MK, Seefeldt LC, Peters JW. A conformational mimic of the MgATP-bound "on state" of the nitrogenase iron protein. Biochemistry 2004;43:1787–97. [PubMed: 14967020]
23. Jang SB, Jeong MS, Seefeldt LC, Peters JW. Structural and biochemical implications of single amino acid substitutions in the nucleotide-dependent switch regions of the nitrogenase Fe protein from *Azotobacter vinelandii*. J Biol Inorg Chem 2004;9:1028–33. [PubMed: 15549494]
24. Chiu H, Peters JW, Lanzilotta WN, Ryle MJ, Seefeldt LC, et al. MgATP-bound and nucleotide-free structures of a nitrogenase protein complex between the Leu 127 delta-Fe-protein and the MoFe-protein. Biochemistry 2001;40:641–50. [PubMed: 11170380]
25. Jang SB, Seefeldt LC, Peters JW. Modulating the midpoint potential of the [4Fe-4S] cluster of the nitrogenase Fe protein. Biochemistry 2000;39:641–48. [PubMed: 10651628]
26. Rees DC, Tezcan FA, Haynes CA, Walton MY, Andrade S, et al. Structural basis of biological nitrogen fixation. Phil Trans R Soc A 2005;363:971–84. [PubMed: 15901546]
27. Howard JB, Rees DC. Structural basis of biological nitrogen fixation. Chem Rev 1996;96:2965–82. [PubMed: 11848848]
28. Howard JB, Rees DC. Nitrogenase: A nucleotide-dependent molecular switch. Annu Rev Biochem 1994;63:235–64. [PubMed: 7979238]
29. Dos Santos PC, Igarashi RY, Lee HI, Hoffman BM, Seefeldt LC, Dean DR. Substrate interactions with the nitrogenase active site. Acc Chem Res 2005;38:208–14. [PubMed: 15766240]
30. Seefeldt LC, Dance I, Dean DR. Substrate interactions with nitrogenase: Fe versus Mo. Biochemistry 2004;43:1401–09. [PubMed: 14769015]
31. Seefeldt LC, Dean DR. Role of nucleotides in nitrogenase catalysis. Acc Chem Res 1997;30:260–66.
32. Hageman RV, Burris RH. Nitrogenase and nitrogenase reductase associate and dissociate with each catalytic cycle. Proc Natl Acad Sci USA 1978;75:2699–702. [PubMed: 275837]
33. Thorneley, RNF.; Lowe, DJ. Molybdenum Enzymes. Spiro, TG., editor. New York: Wiley; 1985. p. 221-84.
34. Lowe, DJ.; Ashby, GA.; Brune, M.; Knights, H.; Webb, MR.; Thorneley, RNF. Nitrogen Fixation: Fundamentals and Applications. Tikhonovich, IA.; Provorov, NA.; Romanov, VI.; Newton, WE., editors. Boston: Kluwer; 1995. p. 103-08.
35. Martin AE, Burgess BK, Iismaa SE, Smartt CT, Jacobson MR, Dean DR. Construction and characterization of an *Azotobacter vinelandii* strain with mutations in the genes encoding flavodoxin and ferredoxin I. J Bacteriol 1989;171:3162–67. [PubMed: 2722744]
36. Mortenson LE. Ferredoxin requirement for nitrogen fixation by extracts of *Clostridium pasteurianum*. Biochim Biophys Acta 1964;81:473–78. [PubMed: 14170319]
37. Thorneley RNF. Nitrogenase of *Klebsiella pneumoniae*: a MgATP hydrolysing energy transduction system with similarities to actomyosin and p21 ras. Philos Trans R Soc London Ser B 1992;336:73–82. [PubMed: 1351299]
38. Wolle D, Dean DR, Howard JB. Nucleotide iron-sulfur cluster signal transduction in the nitrogenase iron-protein: The role of Asp125. Science 1992;258:992–95. [PubMed: 1359643]
39. Ryle MJ, Seefeldt LC. Elucidation of a MgATP signal transduction pathway in the nitrogenase iron protein: Formation of a conformation resembling the MgATP-bound state by protein engineering. Biochemistry 1996;35:4766–75. [PubMed: 8664266]
40. Rees DC, Howard JB. Nitrogenase: standing at the crossroads. Curr Opin Chem Biol 2000;4:559–66. [PubMed: 11006545]
41. Hoover TR, Robertson AD, Cerny RL, Hayes RN, Imperial J, et al. Identification of the V factor needed for the synthesis of the iron-molybdenum cofactor of nitrogenase as homocitrate. Nature 1987;329:855–7. [PubMed: 3313054]
42. Lukoyanov D, Pelmenschikov V, Maeser N, Laryukhin M, Yang TC, et al. Testing if the interstitial atom, X, of the nitrogenase molybdenum-iron cofactor is N or C: ENDOR, ESEEM, and DFT studies of the S = 3/2 resting state in multiple environments. Inorg Chem 2007;46:11437–49. [PubMed: 18027933]

43. Yang TC, Maeser NK, Laryukhin M, Lee HI, Dean DR, et al. The interstitial atom of the nitrogenase FeMo-cofactor: ENDOR and ESEEM evidence that it is not a nitrogen. J Am Chem Soc 2005;127:12804–05. [PubMed: 16159266]
44. Lee HI, Benton PM, Laryukhin M, Igarashi RY, Dean DR, et al. The interstitial atom of the nitrogenase FeMo-cofactor: ENDOR and ESEEM show it is not an exchangeable nitrogen. J Am Chem Soc 2003;125:5604–05. [PubMed: 12733878]
45. Christiansen J, Goodwin PJ, Lanzilotta WN, Seefeldt LC, Dean DR. Catalytic and biophysical properties of a nitrogenase apo-MoFe protein produced by a *nifB*-deletion mutant of *Azotobacter vinelandii*. Biochemistry 1998;37:12611–23. [PubMed: 9730834]
46. Ribbe MW, Hu YL, Guo ML, Schmid B, Burgess BK. The FeMoco-deficient MoFe protein produced by a *nifH* deletion strain of *Azotobacter vinelandii* shows unusual P-cluster features. J Biol Chem 2002;277:23469–76. [PubMed: 11978793]
47. Imperial J, Hoover TR, Madden MS, Ludden PW, Shah VK. Substrate reduction properties of dinitrogenase activated *in vitro* are dependent upon the presence of homocitrate or its analogue during iron-molybdenum cofactor synthesis. Biochemistry 1989;28:7796–99. [PubMed: 2514794]
48. Madden MS, Kindon ND, Ludden PW, Shah VK. Diastereomer-dependent substrate reduction properties of a dinitrogenase containg 1-flourohomocitrate in the iron-molybdenum cofactor. Proc Natl Acad Sci USA 1990;87:6517–21. [PubMed: 2204057]
49. Madden MS, Paustian TD, Ludden PW, Shah VK. Effects of homocitrate, homocitrate lactone, and fluorohomocitrate on nitrogenase in *nifV*- mutants of *Azotobacter vinelandii*. J Bacteriol 1991;173:5403–05. [PubMed: 1885520]
50. Pollock CR, Lee H-I, Cameron LM, DeRose VJ, Hales BJ, et al. Investigation of CO bound to inhibited forms of nitrogenase MoFe protein by ^{13}C ENDOR. J Am Chem Soc 1995;117:8686–87.
51. Christie PD, Lee HI, Cameron LM, Hales BJ, Orme-Johnson WH, Hoffman BM. Identification of the CO-binding cluster in nitrogenase MoFe protein by ENDOR of ^{57}Fe isotopomers. J Am Chem Soc 1996;118:8707–09.
52. Lee HI, Cameron LM, Hales BJ, Hoffman BM. CO binding to the FeMo cofactor of CO-inhibited nitrogenase: ^{13}CO and ^{1}H Q-band ENDOR investigation. J Am Chem Soc 1997;119:10121–26.
53. Lee HI, Cameron LM, Sørlie M, Pollock RC, Christie PD, et al. Study of substrate inhibitor interactions in nitrogenase MoFe protein by advanced paramagnetic resonance. J Inorg Biochem 1999;74:202–02.
54. Lee HI, Hales BJ, Hoffman BM. Metal-ion valencies of the FeMo cofactor in CO-inhibited and resting state nitrogenase by ^{57}Fe Q-band ENDOR. J Am Chem Soc 1997;119:11395–400.
55. Grossman JG, Hasnain SS, Yousafzai FK, Smith BE, Eady RR, et al. Comparing crystallographic and solution structures of nitrogenase complexes. Acta Crystallogr D Biol Crystallogr 1999;55:727–28. [PubMed: 10336305]
56. Rees, DC.; Schindelin, H.; Kisker, C.; Schlessman, J.; Peters, JW., et al. Biological Nitrogen Fixation for the 21st Century. Elmerich, C.; Kondorosi, A.; Newton, WE., editors. Boston: Kluwer Academic Publishers; 1998. p. 11-16.
57. Peters JW, Fisher K, Newton WE, Dean DR. Involvement of the P cluster in intramolecular electron transfer within the nitrogenase MoFe protein. J Biol Chem 1995;270:27007–13. [PubMed: 7592949]
58. Lowe DJ, Fisher K, Thorneley RNF. *Klebsiella pneumoniae* nitrogenase: pre-steady state absorbance changes show that redox changes occur in the MoFe protein that depend on substrate and component protein ratio; a role for P-centres in reducing nitrogen? Biochem J 1993;292:93–98. [PubMed: 8389132]
59. Chan JM, Christiansen J, Dean DR, Seefeldt LC. Spectroscopic evidence for changes in the redox state of the nitrogenase P-cluster during turnover. Biochemistry 1999;38:5779–85. [PubMed: 10231529]
60. Peters JW, Stowell MHB, Soltis SM, Finnegan MG, Johnson MK, Rees DC. Redox-dependent structural changes in the nitrogenase P-cluster. Biochemistry 1997;36:1181–87. [PubMed: 9063865]
61. Yoo SJ, Angove HC, Papaefthymiou V, Burgess BK, Münck E. Mössbauer study of the MoFe protein of nitrogenase from *Azotobacter vinelandii* using selective ^{57}Fe enrichment of the M-centers. J Am Chem Soc 2000;122:4926–36.

62. Lindahl PA, Papaefthymiou V, Orme-Johnson WH, Münck E. Mössbauer studies of solid thionin-oxidized MoFe protein of nitrogenase. J Biol Chem 1988;263:19412–18. [PubMed: 2848826]
63. Hagen WR, Wassink H, Eady RR, Smith BE, Haaker H. Quantitative EPR of an S = 7/2 system in thionine-oxidized MoFe proteins of nitrogenase. A redefinition of the P-cluster concept. Eur J Biochem 1987;169:457–65. [PubMed: 2826146]
64. Pierik AJ, Wassink H, Haaker H, Hagen WR. Redox properties and EPR spectroscopy of the P-clusters of *Azotobacter vinelandii* MoFe protein. Eur J Biochem 1993;212:51–61. [PubMed: 8383042]
65. Lanzilotta WN, Christiansen J, Dean DR, Seefeldt LC. Evidence for coupled electron and proton transfer in the [8Fe-7S] cluster of nitrogenase. Biochemistry 1998;37:11376–84. [PubMed: 9698385]
66. Lanzilotta WN, Seefeldt LC. Changes in the midpoint potentials of the nitrogenase metal centers as a result of iron protein-molybdenum-iron protein complex formation. Biochemistry 1997;36:12976–83. [PubMed: 9335558]
67. Tittsworth RC, Hales BJ. Detection of EPR signals assigned to the 1-equiv-oxidized P-clusters of the nitrogenase MoFe protein from *Azotobacter vinelandii*. J Am Chem Soc 1993;115:9763–67.
68. Lowe DJ, Fisher K, Thorneley RNF. *Klebsiella pneumoniae* nitrogenase: Pre-steady-state absorbance changes show that redox changes occur in the molybdenum-iron protein that depend on substrate and component protein ratio; A role for P-centers in reducing dinitrogen? Biochem J 1993;292:93–98. [PubMed: 8389132]
69. Liang J, Burris RH. Hydrogen burst associated with nitrogenase-catalyzed reactions. Proc Natl Acad Sci USA 1988;85:9446–50. [PubMed: 3200830]
70. Simpson FB, Burris RH. A nitrogen pressure of 50 atmoshperes does not prevent evolution of hydrogen by nitrogenase. Science 1984;224:1095–97. [PubMed: 6585956]
71. Dilworth MJ. Acetylene reduction by nitrogen-fixing prepartions from Clostridium pasteurianum. Biochim Biophys Acta 1966;127:285–94. [PubMed: 5964974]
72. Smith BE, Durrant MC, Fairhurst SA, Gormal CA, Gronberg KLC, et al. Exploring the reactivity of the isolated iron-molybdenum cofactor of nitrogenase. Coord Chem Rev 1999;185–186:669–87.
73. Kim CH, Newton WE, Dean DR. Role of the MoFe protein alpha-subunit histidine-195 residue in FeMo-cofactor binding and nitrogenase catalysis. Biochemistry 1995;34:2798–808. [PubMed: 7893691]
74. Thomann H, Bernardo M, Newton WE, Dean DR. N coordination of MoFe cofactor requires His-195 of the MoFe protein α subunit and is essential for biological nitrogen fixation. Proc Natl Acad Sci USA 1991;88:6620–23. [PubMed: 11607203]
75. Scott DJ, May HD, Newton WE, Brigle KE, Dean DR. Role for the nitrogenase MoFe protein α-subunit in FeMo-cofactor binding and catalysis. Nature 1990;343:188–90. [PubMed: 2153269]
76. Dilworth MJ, Fisher K, Kim CH, Newton WE. Effects on substrate reduction of substitution of histidine-195 by glutamine in the alpha-subunit of the MoFe protein of *Azotobacter vinelandii* nitrogenase. Biochemistry 1998;37:17495–505. [PubMed: 9860864]
77. Fisher K, Dilworth MJ, Newton WE. Differential effects on N_2 binding and reduction, HD formation, and azide reduction with alpha-195His- and alpha-191Gln-substituted MoFe proteins of *Azotobacter vinelandii* nitrogenase. Biochemistry 2000;39:15570–77. [PubMed: 11112544]
78. Christiansen J, Cash VL, Seefeldt LC, Dean DR. Isolation and characterization of an acetylene-resistant nitrogenase. J Biol Chem 2000;275:11459–64. [PubMed: 10753963]
79. Christiansen J, Seefeldt LC, Dean DR. Competitive substrate and inhibitor interactions at the physiologically relevant active site of nitrogenase. J Biol Chem 2000;275:36104–07. [PubMed: 10948195]
80. Lee HI, Igarashi RY, Laryukhin M, Doan PE, Dos Santos PC, et al. An organometallic intermediate during alkyne reduction by nitrogenase. J Am Chem Soc 2004;126:9563–69. [PubMed: 15291559]
81. Igarashi RY, Dos Santos PC, Niehaus WG, Dance IG, Dean DR, Seefeldt LC. Localization of a catalytic intermediate bound to the FeMo-cofactor of nitrogenase. J Biol Chem 2004;279:34770–75. [PubMed: 15181010]
82. Barney BM, Igarashi RY, Dos Santos PC, Dean DR, Seefeldt LC. Substrate interaction at an iron-sulfur face of the FeMo-cofactor during nitrogenase catalysis. J Biol Chem 2004;279:53621–24. [PubMed: 15465817]

83. Benton PMC, Laryukhin M, Mayer SM, Hoffman BM, Dean DR, Seefeldt LC. Localization of a substrate binding site on FeMo-cofactor in nitrogenase: trapping propargyl alcohol with an α-70-substituted MoFe protein. Biochemistry 2003;42:9102–09. [PubMed: 12885243]
84. Dos Santos PC, Mayer SM, Barney BM, Seefeldt LC, Dean DR. Alkyne substrate interaction within the nitrogenase MoFe protein. J Inorg Biochem 2007;101:1642–48. [PubMed: 17610955]
85. Benton PMC, Mayer SM, Shao JL, Hoffman BM, Dean DR, Seefeldt LC. Interaction of acetylene and cyanide with the resting state of nitrogenase alpha-96-substituted MoFe proteins. Biochemistry 2001;40:13816–25. [PubMed: 11705370]
86. Barney BM, Laryukhin M, Igarashi RY, Lee HI, Dos Santos PC, et al. Trapping a hydrazine reduction intermediate on the nitrogenase active site. Biochemistry 2005;44:8030–37. [PubMed: 15924422]
87. Igarashi RY, Laryukhin M, Dos Santos PC, Lee HI, Dean DR, et al. Trapping H^- bound to the nitrogenase FeMo-cofactor active site during H_2 evolution: characterization by ENDOR spectroscopy. J Am Chem Soc 2004;127:6231–41. [PubMed: 15853328]
88. Davis LC, Henzl MT, Burris RH, Orme-Johnson WH. Iron-sulfur clusters in the molybdenum-iron protein component of nitrogenase. Electron paramagnetic resonance of the carbon monoxide inhibited state. Biochemistry 1979;18:4860–69. [PubMed: 228701]
89. Hwang JC, Chen CH, Burris RH. Inhibition of nitrogenase-catalyzed reductions. Biochim Biophys Acta 1973;292:256–70. [PubMed: 4705133]
90. Cameron LM, Hales BJ. Investigation of CO binding and release from Mo-nitrogenase during catalytic turnover. Biochemistry 1998;37:9449–56. [PubMed: 9649328]
91. Lee HI, Sørlie M, Christiansen J, Yang TC, Shao J, et al. Electron inventory, kinetic assignment (E(n)), structure, and bonding of nitrogenase turnover intermediates with C_2H_2 and CO. J Am Chem Soc 2005;127:15880–90. [PubMed: 16277531]
92. Burris RH. Nitrogenase. J Biol Chem 1991;266:9339–42. [PubMed: 1903384]
93. Thorneley RNF, Eady RR, Lowe DJ. Biological nitrogen fixation by way of an enzyme-bound dinitrogen-hydride intermediate. Nature 1978;272:557–58.
94. Barney BM, Lukoyanov D, Yang TC, Dean DR, Hoffman BM, Seefeldt LC. A methyldiazene ($HN=N-CH_3$) derived species bound to the nitrogenase active site FeMo-cofactor: implications for mechanism. Proc Natl Acad Sci USA 2006;103:17113–18. [PubMed: 17088552]
95. Barney BM, McClead J, Lukoyanov D, Laryukhin M, Yang TC, et al. Diazene (HN=NH) is a substrate for nitrogenase: insights into the pathway of N_2 reduction. Biochemistry 2007;46:6784–94. [PubMed: 17508723]
96. Pickett CJ. The Chatt cycle and the mechanism of enzymic reduction of molecular nitrogen. J Biol Inorg Chem 1996;1:601–06.
97. Chatt J, Dilworth JR, Richards RL. Recent advances in the chemistry of nitrogen fixation. Chem Rev 1978;78:589–625.
98. Yandulov DV, Schrock RR. Catalytic reduction of dinitrogen to ammonia at a single molybdenum center. Science 2003;301:76–78. [PubMed: 12843387]
99. Schrock RR. Catalytic reduction of dinitrogen under mild conditions. Chem Commun 2003:2389–91.
100. Schrock RR. Catalytic reduction of dinitrogen to ammonia at well defined single metal sites. Phil Trans R Soc A 2005;363:959–69. [PubMed: 15901545]
101. Schrock RR. Catalytic reduction of dinitrogen to ammonia by molybdenum: theory versus experiment. Angew Chem Int Ed Engl 2008;47:5512–22. [PubMed: 18537212]
102. Weare WW, Dai X, Byrnes MJ, Chin JM, Schrock RR, Muller P. Catalytic reduction of dinitrogen to ammonia at a single molybdenum center. Proc Natl Acad Sci U S A 2006;103:17099–106. [PubMed: 17085586]
103. Barney BM, Yang TC, Igarashi RY, Dos Santos PC, Laryukhin M, et al. Intermediates trapped during nitrogenase reduction of N_2, $CH_3-N=NH$, and H_2N-NH_2. J Am Chem Soc 2005;127:14960–61. [PubMed: 16248599]
104. Davis LC. Hydrazine as a substrate and inhibitor of *Azotobacter vinelandii* nitrogenase. Arch Biochem Biophys 1980;204:270–76. [PubMed: 6932825]

105. Lukoyanov D, Barney BM, Dean DR, Seefeldt LC, Hoffman BM. Connecting nitrogenase intermediates with the N_2 reduction kinetic scheme by a relaxation protocol and identification of the N_2 binding state. Proc Natl Acad Sci USA 2007;104:1451–55. [PubMed: 17251348]

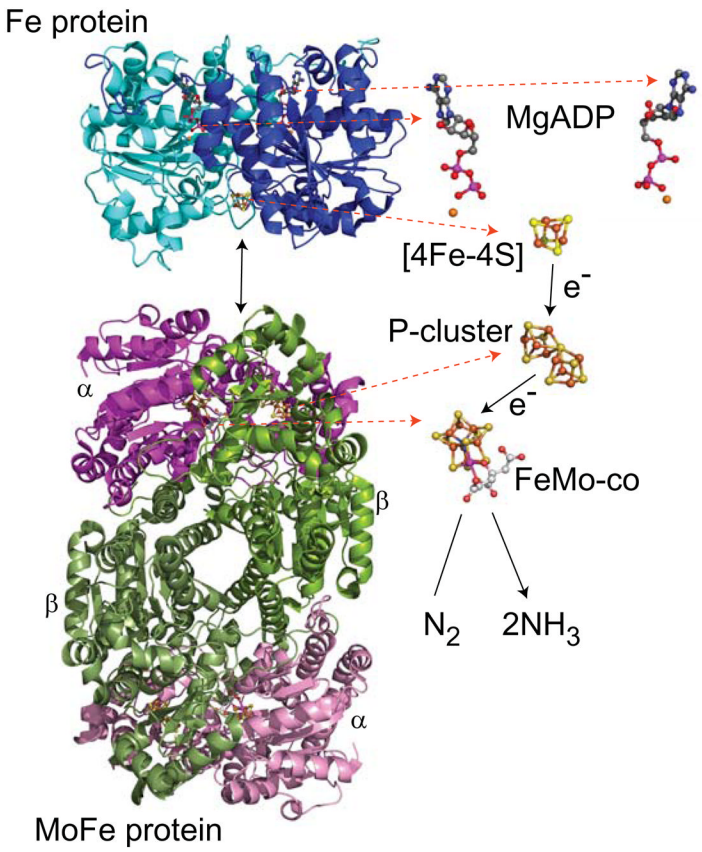

Figure 1.

Structures of the nitrogenase MoFe and Fe proteins. The MoFe protein is an $\alpha_2\beta_2$ tetramer, with the alpha subunits shown in magenta and the beta subunits shown in green. The Fe protein is a γ_2 dimer, with each subunit shown in blue. A MoFe protein binds two Fe proteins, with each αβ unit being a catalytic unit. One Fe protein is shown associating with one αβ-unit of the MoFe protein. The relative positions and structures of two bound MgADP molecules, the Fe protein [4Fe-4S] cluster, and MoFe protein P-cluster (8Fe-7S), and FeMo-cofactor (7Fe-Mo-9S-homocitrate-X) are shown. Each is highlighted to the right. The flow of electrons is from the [4Fe-4S] cluster to the P-cluster to the FeMo-cofactor. The element color scheme is C in gray, O is red, N in blue, Fe in rust, S in yellow, and Mo in magenta. Graphics were generated with the program Pymol using the Protein Data Base (PDB) files 1M1N for the MoFe protein and 1FP6 for the Fe protein.

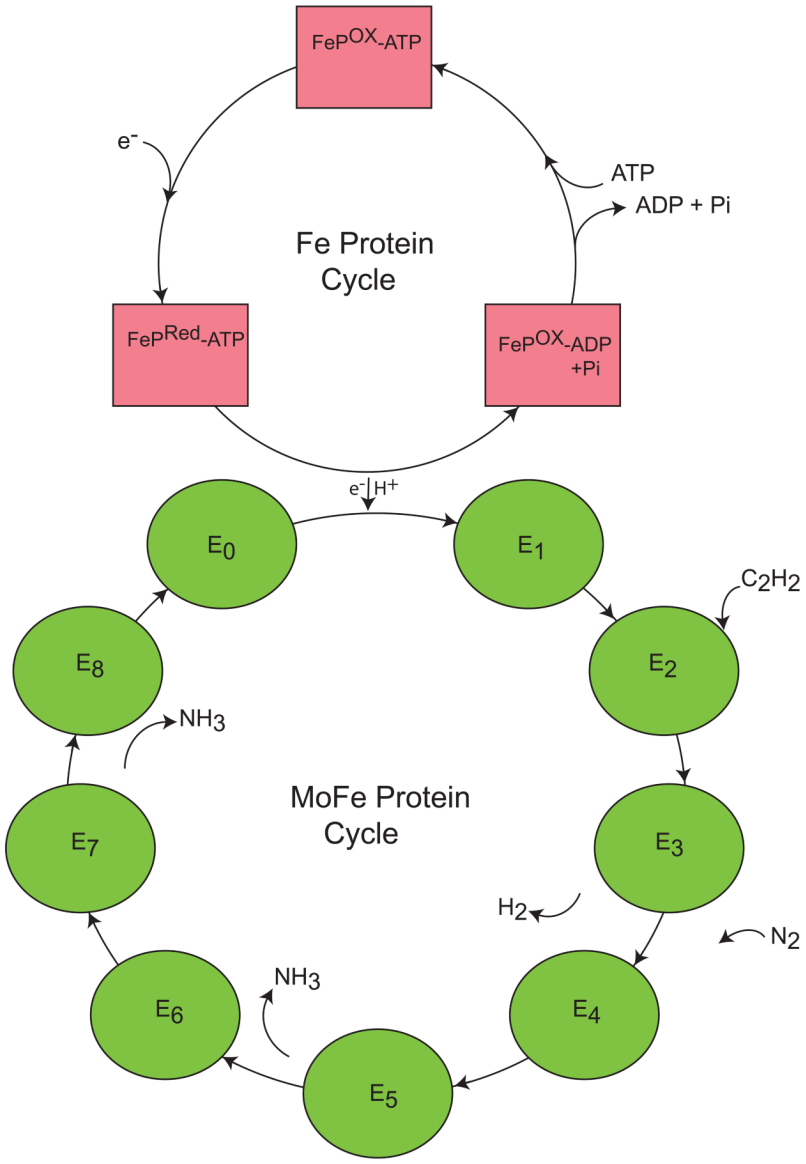

Figure 2.

Fe and MoFe protein catalytic cycles. Shown is a three state cycle for the Fe protein (top) and an eight state cycle for the MoFe protein (bottom). For the Fe protein (abbreviated FeP), the [4Fe-4S] cluster can exist in the +1 reduced state (Red) or the 2+ oxidized state (Ox). The Fe protein either has two MgATP molecules bound (ATP) or two MgADP with two Pi (ADP+Pi). The exchange of an electron occurs upon association of the Fe protein with the MoFe protein at the bottom of the cycle. In the MoFe protein cycle, the MoFe protein is successively reduced by one electron, with reduced states represented by E_n, where n is the total number of electrons donated by the Fe protein. Acetylene (C_2H_2) is shown binding to E_2, while N_2 is shown binding to E_3 and E_4. N_2 binding is accompanied by the displacement of H_2. The two ammonia molecules are shown being liberated from later E states.

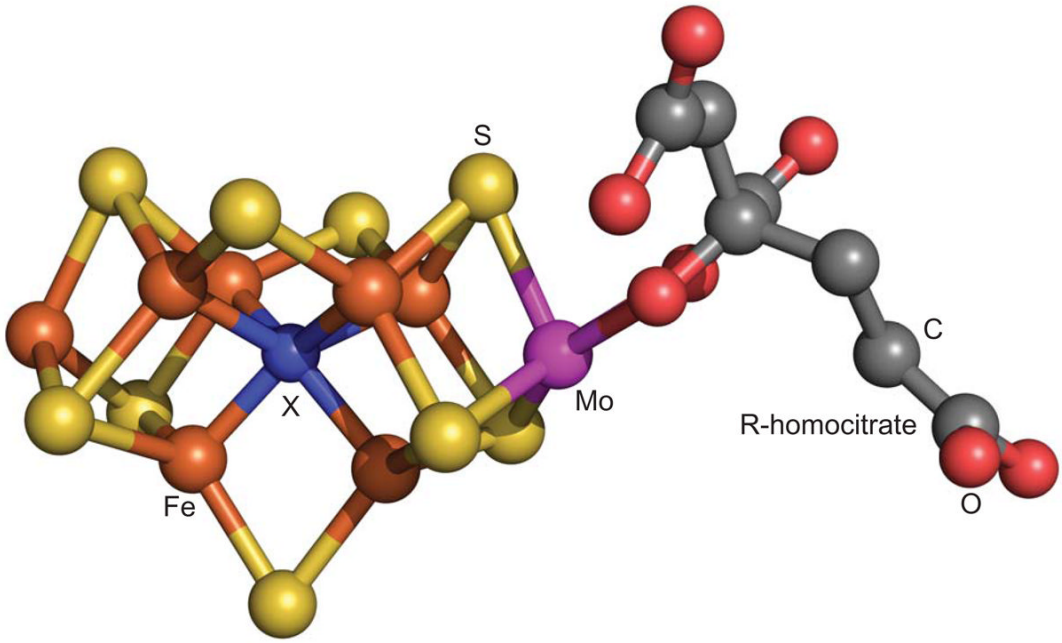

Figure 3.
Structure of the FeMo-cofactor of nitrogenase. The element colors are as described in the legend to Figure 1.

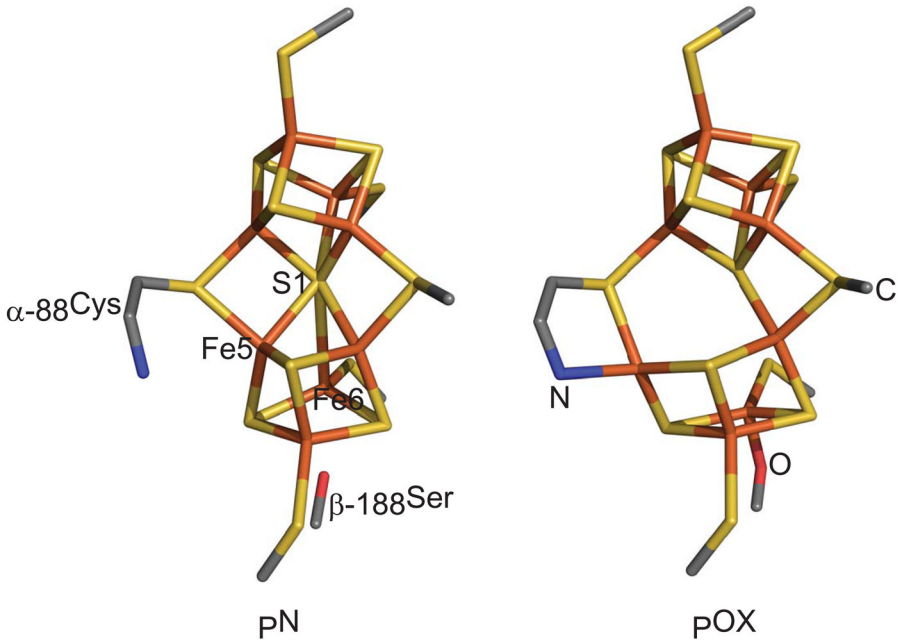

Figure 4.

P-cluster structures. Shown are the structures of the P-cluster [8Fe-7S] in the oxidized (P^{ox}) and reduced (P^{N}) states. MoFe protein amino acid ligands are also shown with β-188^{Ser} and α-88^{Cys} labeled. The central S atom is labeled S1. The PBD files used were 2MIN for the P^{ox} state and 3MIN for the P^{N} state.

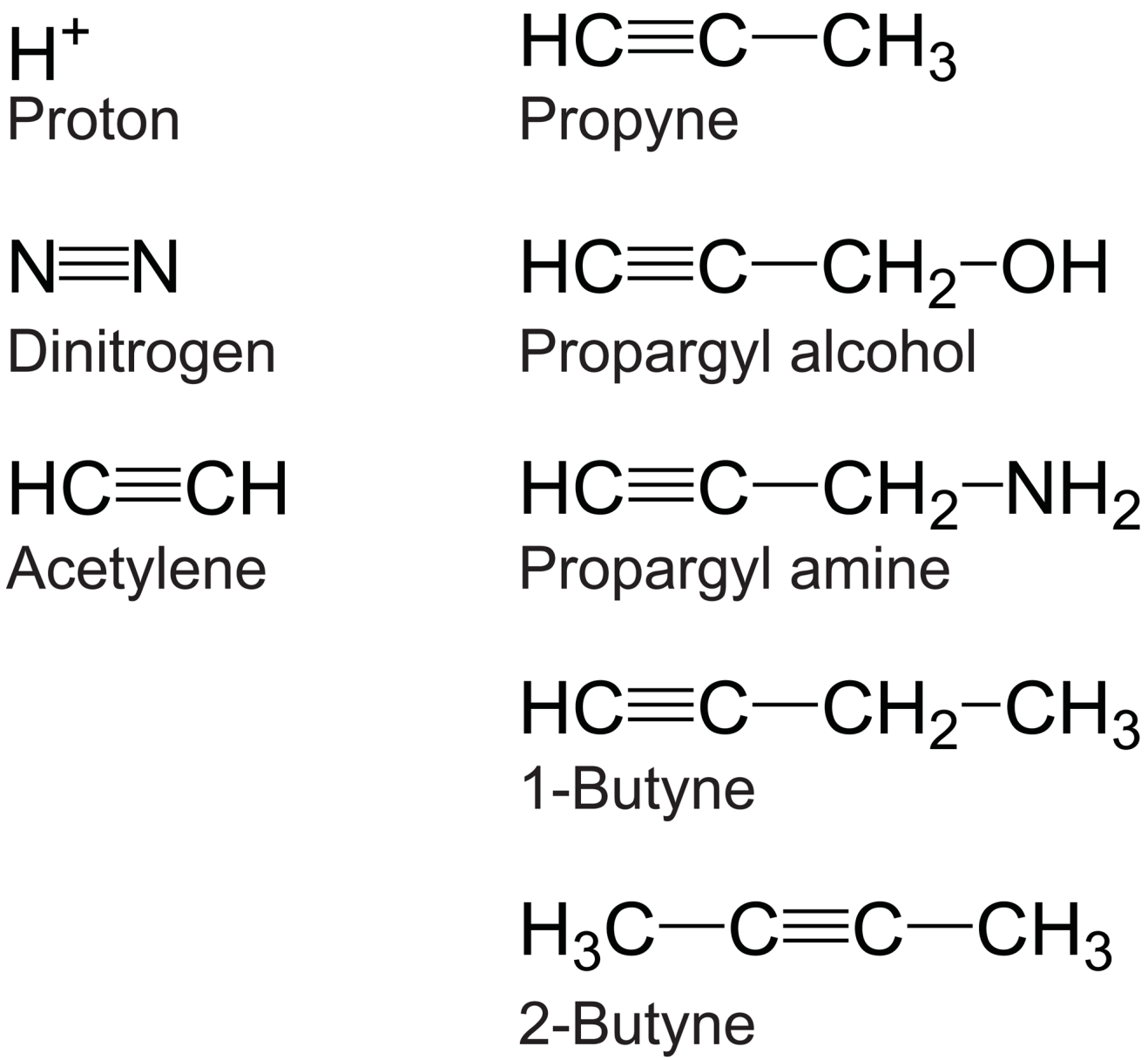

Figure 5.
Substrates for nitrogenase. Shown are the structures for select nitrogenase substrates. Compounds that are substrates for the wild-type enzyme are shown to the left, while compounds that become substrate for MoFe proteins with amino acid substitutions for α-70^{Val} are shown to the right.

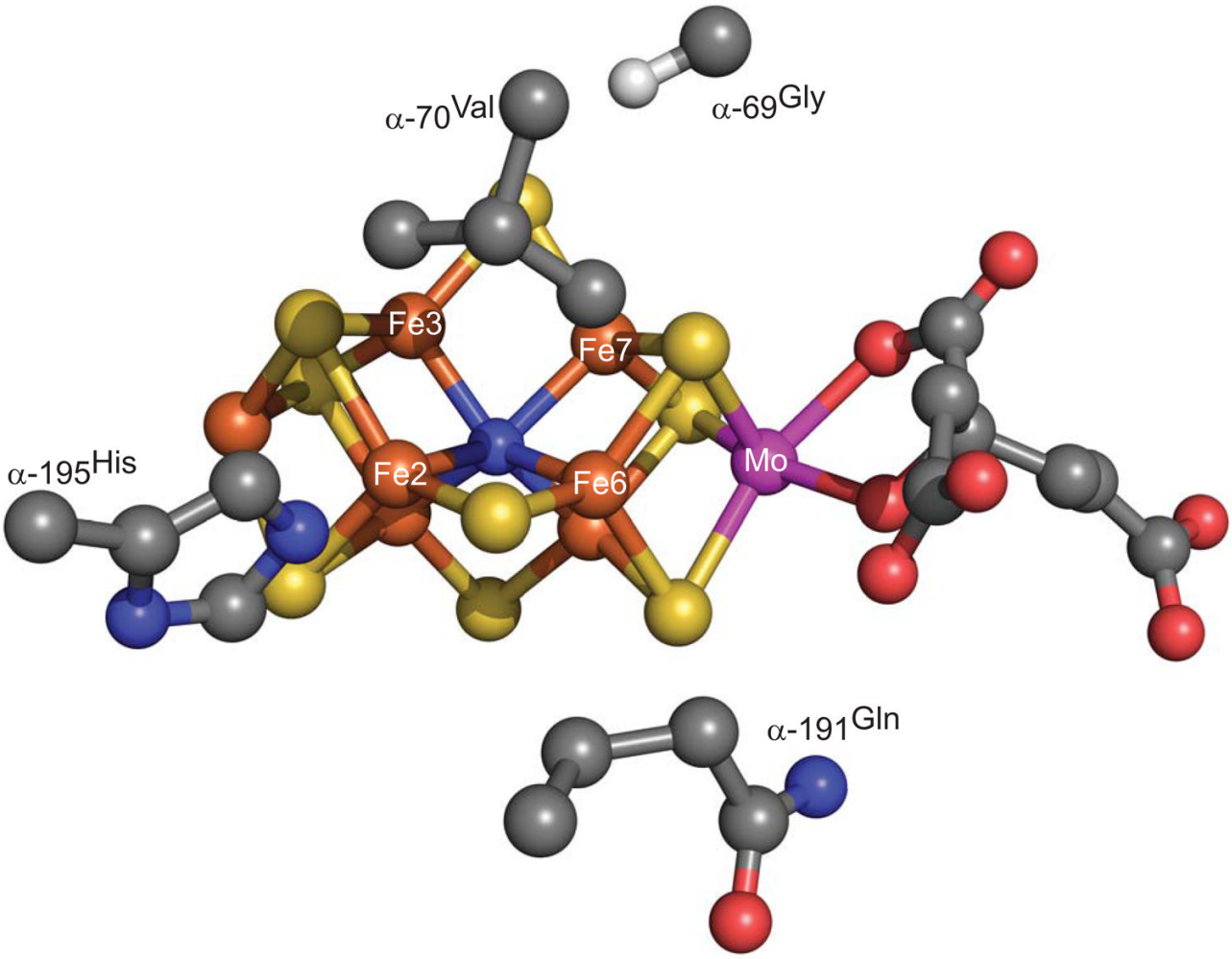

Figure 6.
Substrate binding location on FeMo-cofactor. Shown is the FeMo-cofactor with Fe atoms 2, 3, 6, and 7 labeled. The view is from the top looking down on the Fe face that binds substrates. Carbon alpha and the side chain are shown for α-69^{Gly}, α-70^{Val}, α-195^{His}, and α-191^{Gln}. PDB file 1M1N.

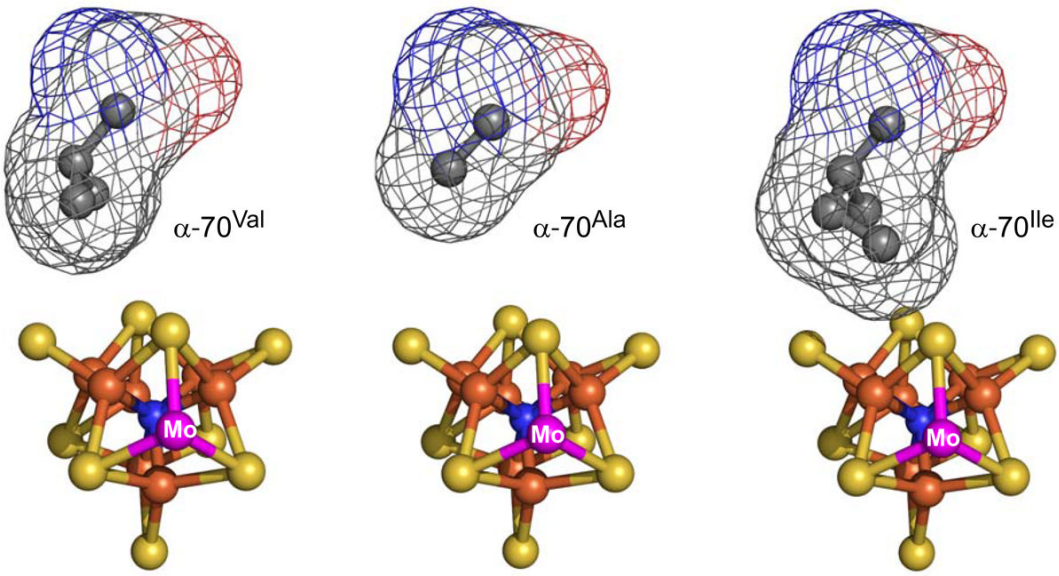

Figure 7.
Control of substrate access to FeMo-cofactor. Shown is the FeMo-cofactor without R-homocitrate viewed down the Mo end. The side chain of α-70^{Val} is shown with a Van der Waals mesh (left). Also shown are computer generated models of the Van der Waals surface for α-70^{Ala} (center) and α-70^{Ile} (right) substituted MoFe proteins.

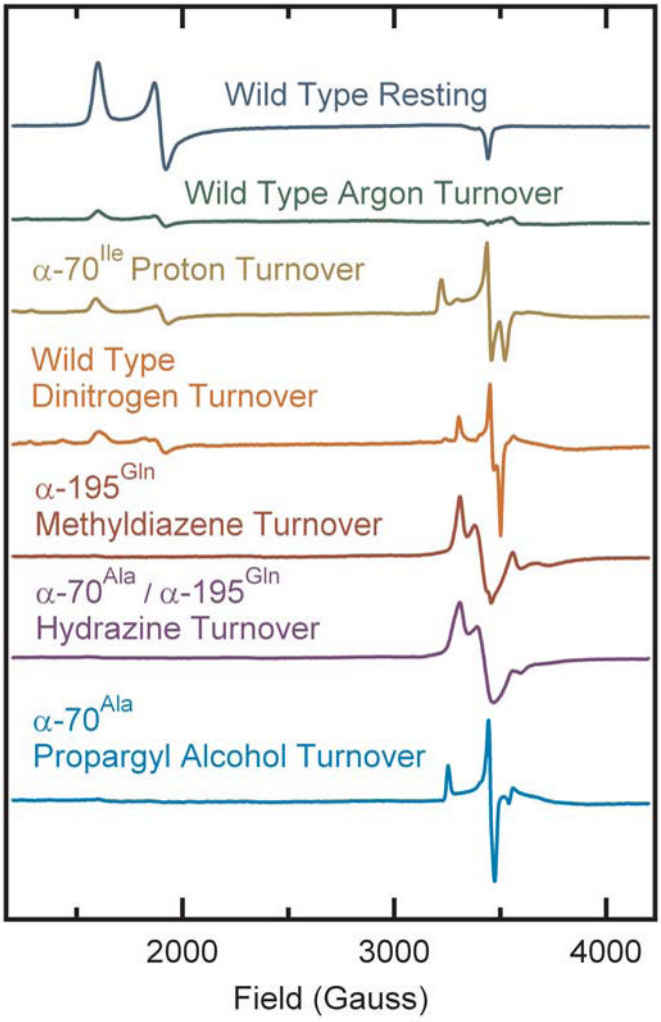

Figure 8.

EPR spectra of nitrogenase with trapped substrates. Shown are EPR spectra for various MoFe protein variants that were frozen in liquid nitrogen either in the resting state (top spectrum) or during steady state turnover (all other spectra) in the presence of different substrates. The MoFe protein and substrate is noted on each spectrum. EPR spectra were acquired between 8–12 K.

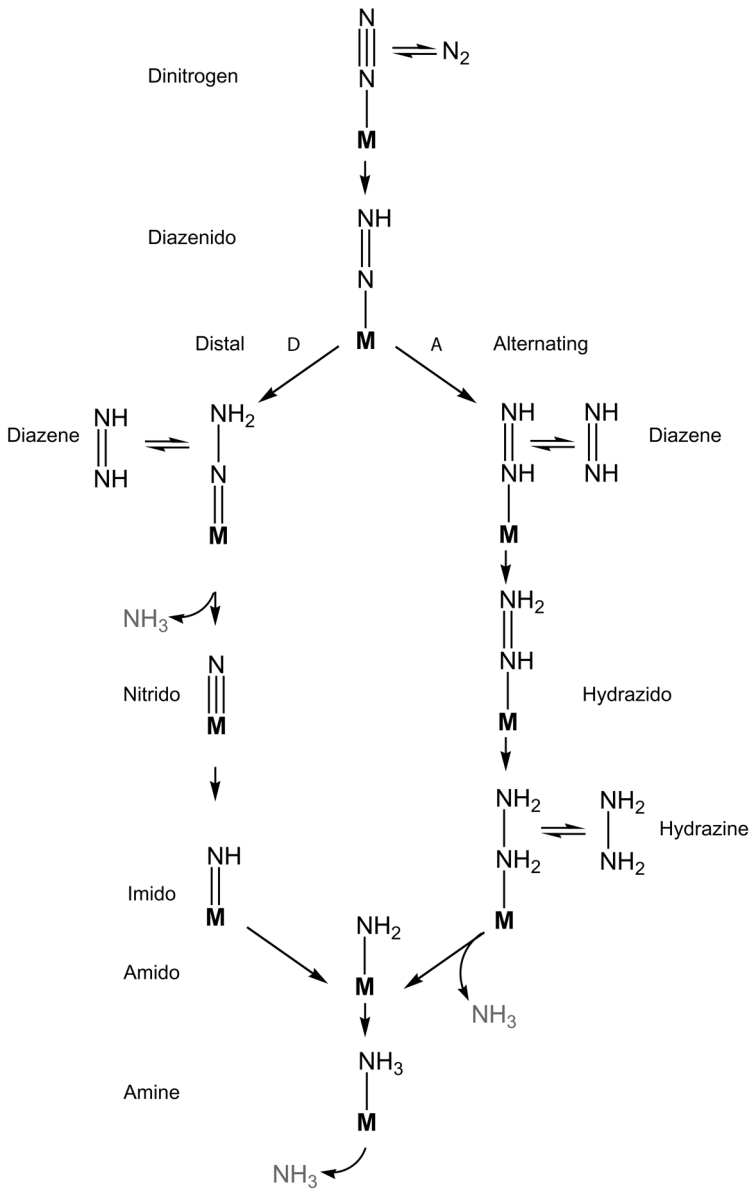

Figure 9.

Possible reaction mechanisms for nitrogenase. Shown are two possible reaction mechanisms for nitrogenase. On the left is shown the distal mechanism and on the right the alternating mechanism. FeMo-cofactor is abbreviated as M and the names of different bound states are shown. Possible points of entry for diazene and hydrazine are shown.